Raise Your Voice at a Proper Pace to Synchronize in Multiple *Ad Hoc* Piconets

Xiliang Luo, *Member, IEEE*, and Georgios B. Giannakis, *Fellow, IEEE*

Abstract—Timing synchronization of symbol boundaries is known to affect critically the performance of all coherent communication systems. Its effects are particularly pronounced in contemporary wireless technologies including ultrawideband (UWB) radios and wireless sensor networks (WSNs), where cooperative or *ad hoc* access is challenged by arbitrary asynchronism, intersymbol interference (ISI), receiver noise, as well as inter and intrapiconet interference arising from concurrently communicating nodes. To cope with these challenges, this paper introduces piconet-specific synchronization patterns and simple averaging operations at the receiving ends, which enable low-complexity timing acquisition through energy detection and demodulation by matching to a synchronized aggregate template (SAT). Pattern sequences are designed for both training-based and blind operation. Either way, the idea behind these designs is to periodically increase the transmit-power ("voice") of each piconet's synchronizing node with a period ("pace") characteristic of each piconet. Performance of the novel synchronization protocols is tested with simulations conforming to an UWB wireless personal area network (WPAN) setup.

Index Terms—Synchronization, ultrawideband (UWB), wireless personal area network (WPAN), wireless sensor network (WSN).

NOMENCLATURE

$\lceil \cdot \rceil$	Integer ceiling.
$\lfloor \cdot \rfloor$	Floor operations.
$\mathsf{E}[\cdot]$	Expectation.
$\star$	Linear convolution.
$\mathbb{N}$	Set of natural numbers.
$\mathbb{Z}$	Set of integers.
$\delta[\cdot]$	Kronecker delta.
$\delta(\cdot)$	Dirac delta.

I. INTRODUCTION

TIMING synchronization of symbol boundaries is a performance-critical factor at the physical layer of all coherent communication systems: From classical narrowband (NB) and emerging ultrawideband (UWB) radios to cooperative relay-communications, wireless sensor networks (WSNs), distributed localization, and clustering and routing; see, e.g., [1], [10], [18], and references therein. Besides additive white Gaussian noise (AWGN) at the receiver, timing algorithms face one or more of the following challenges: 1) intersymbol interference (ISI) induced by frequency-selective multipath propagation; 2) multiuser interference (MUI) arising from concurrent communications within the piconet (or cell) of interest as well as from neighboring piconets; and 3) *ad hoc* access allowing for arbitrarily large delays (unbounded asynchronism) among multiple communicating nodes. Being the first module of any coherent receiver renders the task of symbol timing nearly formidable because ISI-inducing channels and spreading codes (that could be used for coping with MUI) are *unknown* during the synchronization phase.

Synchronization challenges are magnified in UWB radios even for single-user point-to-point links where ISI effects are particularly pronounced, causing bit error rate (BER) performance to degrade severely due to mistiming [16], and capacity to diminish when timing offset as well as channel coefficients and tap delays cannot be acquired [12]. MUI is also severe in UWB links envisioned for wireless indoor multipiconet access [5], and potentially for low-power WSNs outdoors [11]. Most UWB synchronizers rely on training, and some assume absence of interframe interference and ISI [3], or sampling rates as high as several gigahertz [6]. The innovation rate sampling in [9] can afford analog-to-digital converters of pragmatic speed but cannot handle MUI and becomes increasingly complex in *ad hoc* operation. Existing blind alternatives have either relied on the transmitted-reference scheme to bypass channel estimation at the expense of bandwidth loss in the absence of ISI [2], or utilize the nonzero-mean property of pulse position modulated transmissions to estimate a single-user channel in the absence of MUI [17]. The timing with dirty templates (TDT) approach in [19] can cope with interframe interference without bandwidth loss, but does not allow for ISI especially when MUI is also present.

The blind scheme in [7] on the other hand, comes with a number of attractive features, as follows: universal applicability to NB, WB, or UWB systems; resilience to AWGN, interframe interference, and ISI without bandwidth loss; analog or digital implementation with affordable complexity; and robustness to MUI provided that the node-seeking timing acquisition receives

only a single synchronization signal. The latter is reasonable when considering *ad hoc* access in a single UWB piconet with a single master node, or, when the base station in a fixed access cellular setting synchronizes mobile stations. Besides blind timing acquisition, the approach in [7] enables decision-directed tracking and low-complexity demodulation based on what is termed synchronized aggregate template (SAT). Detailed performance analysis shows that SAT-based demodulation offers a number of advantages when compared to the popular RAKE reception [8].

The main theme of this paper is timing synchronization of symbol boundaries in multiple *ad hoc* piconets. To this end, we first derive a novel training-based synchronization protocol for *ad hoc* access in a single piconet and unify it with its blind counterpart in [7] (Section II). This unification permeates to the training approach, all attractive features of the blind scheme, including low-complexity SAT-based demodulation. Relative to blind schemes, training consumes bandwidth but has complementary merits in high speed and reliability of acquisition. The second major contribution of this paper concerns the challenging multipiconet scenario, where nodes are allowed to communicate in the presence of AWGN, ISI, and MUI arising from both interpiconet as well as intrapiconet interference (Section III). For both training-based as well as blind modes, we design piconet-specific synchronization patterns and simple averaging operations at the receiving nodes in order to suppress the sources of interference present and enable low-complexity timing acquisition and SAT-based demodulation. Although the development of our analytical results in continuous-time suggests readily analog implementation, we show that all receiver processing can also be performed digitally (Section IV). Performance of our synchronization and demodulation algorithms is tested with simulations conforming to an UWB wireless personal area network (WPAN) setting (Section V). Finally, we wrap up this paper with conclusions in Section VI.

II. SYNCHRONIZATION WITHIN A SINGLE PICONET

In this section, we lay out the channel model as well as transmit–receive operating conditions based on which we derive timing synchronization and demodulation algorithms for a WPAN with a *single* piconet; see also Fig. 1. One node (but not necessarily the same one all the time) is designated to be the piconet's "master" node who is responsible for broadcasting intermittently a pattern for the rest of the ("slave") nodes in the piconet to synchronize. Such a pattern was derived in [7] to enable low-complexity *blind* timing acquisition, tracking, and demodulation. Blind synchronizers and demodulators are attractive when the traffic is continuous as in, e.g., high-definition television (HDTV) broadcasting. In bursty links however, e.g., those encountered with packet switched networks, *training*-based alternatives are preferable for their high speed and performance. Apart from briefly reviewing the blind scheme of [7], we introduce in this section a simple training pattern to obtain a *unified* synchronization and demodulation approach in a single piconet with a single master. The scheme is not only useful on its own, but also paves the way for tackling the challenging generalization to multiple piconets we pursue in Section III.
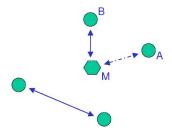

Fig. 1. WPAN comprising a single piconet.

A. System Model

Suppose that the master node broadcasts the binary modulated waveform

$$x(t) = \sqrt{\mathcal{E}} \sum_n s[n] p_T(t - nT_s) \qquad (1)$$

where $\{s[n] = \pm 1\}$ are binary symbols and $p_T(t)$ is the *transmitted* symbol waveform. This transmission can be NB, WB, or UWB [7]. For UWB systems, $p_T(t) = \sum_{k=0}^{N_f-1} p(t - kT_f - c_k T_c)$, where $p(t)$ denotes the normalized ultrashort pulse of duration T_p, i.e., $\int_0^{T_p} p^2(t) dt = 1$, T_f is the frame period, N_f is the number of frames per symbol period $T_s (\geq N_f T_f)$, $\{c_k\}_{k=0}^{N_f-1}$ is the time-hopping (TH) code which enables separation of multiple users, and T_c is the chip period. Typically, the frame period is N_c times the chip period, i.e., $T_f = N_c T_c$ and $c_k \in [0, N_c - 1]$ with $N_c \in \mathbb{N}$. Each pulse $p(t)$ is scaled by $\sqrt{\mathcal{E}}$, so that the transmitted energy per pulse is $\mathcal{E}$.

The multipath channel between any two nodes (here between the master node and a slave node) adheres to a block fading tapped delay line model with $L + 1$ taps (paths)

$$h(t) = \sum_{l=0}^{L} \alpha_l \delta(t - \tau_{l,0} - \tau_0) \qquad (2)$$

where α_l is the real-valued coefficient of path l, $\tau_{l,0}$ is the time delay of path l relative to path 0, and τ_0 denotes the time delay of the first path. Without loss of generality (w.l.o.g.), we consider $\tau_{0,0} \leq \tau_{1,0} \leq \cdots \leq \tau_{L,0}$. All channel parameters are assumed invariant over a block of duration equal to the channel coherence period T_{coh}, but are allowed to change independently from block to block. For typical UWB channels [4], we have $T_{\text{coh}} \gg T_s$.

Within one coherence period T_{coh}, the master's signal received at any slave node in the presence of additive Gaussian noise (AGN), $\eta(t)$, and multiuser interference (MUI) $\rho(t)$ from other slave-to-slave communications, can be expressed as ($\star$ denotes linear convolution)

$$r(t) = x(t) \star h(t) \star \tilde{p}(t) + \rho(t) + \eta(t) \qquad (3)$$

where $\tilde{p}(t)$ is the normalized receive filter with $\int_0^{T_p} \tilde{p}^2(t) dt = 1$. Upon defining the *receive* symbol waveform as $p_R(t) := p_T(t) \star h(t + \tau_0) \star \tilde{p}(t)$, we can rewrite (3) as

$$r(t) = \sqrt{\mathcal{E}} \sum_n s[n] p_R(t - nT_s - \tau_0) + \rho(t) + \eta(t) \qquad (4)$$

where τ_0 is the parameter we wish to estimate during the timing acquisition phase.

If we let $T_R := \sup\{t | p_R(t) \neq 0\}$ denote the nonzero support of $p_R(t)$ and we select the symbol period $T_s \geq T_R$, then the shifted $p_R(t)$ replicas in (4) are separated in time and ISI does not show up in $r(t)$. However, higher data rates become possible as T_s becomes smaller, which gives rise to ISI. Given $r(t)$ and with ISI present or absent, we seek a synchronization pattern leading to low-complexity training-based or blind estimation of τ_0 and $p_R(t)$. To this end, we adopt the following operating conditions.

C0) We select the symbol period so that $T_s > \Delta\tau_{\max} - T_T$, where $\Delta\tau_{\max} \geq \max_{l\in[1,L]}(\tau_{l,0} - \tau_{l-1,0})$ denotes a known upper bound on successive path delay differences, and T_T denotes the nonzero support of $p_T(t) \star \tilde{p}(t)$; we assume throughout that drifts in T_s are negligible.

C1) With an upper bound on the delay spread $\tau_{L,0}$ (and thus T_R) known, we select an integer $M := \lceil T_R/T_s \rceil + 1$.

C2) Except for the symbols involved in the sync pattern which is intermittently broadcasted only from the master node, all other symbols are zero-mean, i.e., $\mathsf{E}[s[n]] = 0$.

C3-T1) The master's "training sync pattern" is a deterministic periodic sequence with each period of size M comprising one symbol equal to 1 followed by $M-1$ zero symbols, i.e., $s[n] = \sum_k \delta[n - kM]$.

C3-B1) The master's "blind sync pattern" consists of one nonzero-mean symbol every $M-1$ zero-mean symbols. The corresponding stream of symbols $\{s[n]\}$ taking values from a finite alphabet equiprobably obeys: $\mathsf{E}[s[n]] = \theta \sum_k \delta[n - kM]$ with $\theta \neq 0$, i.e., the mean of the blind sync pattern coincides (up to a scale) with the deterministic sync pattern under C3-T1).

C4) MUI and AGN in (4) are zero mean, i.e., $\mathsf{E}[\rho(t)] = \mathsf{E}[\eta(t)] = 0$.

Condition C0) is included for mathematical rigor to ensure that over the $[0, T_R]$ support of $p_R(t)$, possible intervals where $p_R(t) = 0$ are no larger than T_s. It is satisfied easily in practice especially since multipath in UWB links is dense. The upper bound on the delay spread required by C1), can be made readily available through sounding experiments. Communicating outside the synchronization phase with zero-mean symbols [as per C2)] is typical for power efficiency reasons. Notice that the sync phase where C3) allows for nonzero-mean symbols lasts for a very small fraction of time. Since MUI comes from zero-mean communications among already synchronized slave nodes, C4) is satisfied because of C2).

The nonzero-mean pattern under C3-B1) can be easily effected by minimally biasing the amplitude of certain constellation points. For instance, we can draw asymmetric BPSK symbols taking values $2\theta + 1$ or -1 equiprobably with nonzero-mean: $\mathsf{E}[s(kM)] = \theta$, where $\theta > 0$. This nonzero-mean pattern is related to the superimposed training used by [20] for blind estimation of discrete-time point-to-point channels, but is more desirable in our multiaccess synchronization–demodulation context; see [7] and [8] for more details on this relationship and for extensions to general linear (e.g., quadrature amplitude) and nonlinear (e.g., pulse position) modulations.
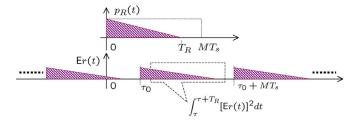

Fig. 2. Schematic illustrating the energy detector used in Theorem 1 for timing estimation.

B. Synchronization and Template Recovery

If the master node broadcasts the deterministic sync pattern $s[n] = \sum_k \delta[n - kM]$ as in C3-T1), the waveform received by any slave node can be written as [cf. (4)]

$$r(t) = \sqrt{\mathcal{E}} \sum_k p_R(t - kMT_s - \tau_0) + \rho(t) + \eta(t). \quad (5)$$

Taking expectation on both sides of (5), we find $\mathsf{E}r(t) = \sqrt{\mathcal{E}} \sum_k p_R(t - kMT_s - \tau_0)$. If we now consider any $\mathsf{E}r(t)$ segment of size MT_s, the $p_R(t)$ replica that falls into it will be circularly shifted by τ_0. On the other hand, consecutive $p_R(t)$ replicas in (5) are separated by more than T_s, since $MT_s - T_R \geq T_s$ under C2); see also Fig. 2. This guard time which has size at least T_s seconds, allows one to resolve the circular shift and thus recover τ_0.

Interestingly, we arrive (within a scale θ) at the same expression for $\mathsf{E}r(t)$, if we take expectation on both sides of (4) and adopt the pattern C3-B1) for which $\mathsf{E}s[n] = \theta \sum_k \delta[n - kM]$. This observation establishes that similar to [7] which relied on C3-B1), even with the training pattern in C3-T1), the unknown timing offset τ_0 can be recovered using a low-complexity energy detector as

$$\tau_0 = \arg \max_{\tau\in[0,MT_s)} \int_\tau^{\tau+T_R} [\mathsf{E}r(t)]^2 dt. \quad (6)$$

With τ_0 available, the SAT of the received symbol waveform can also be found as $p_R(t) = (1/\sqrt{\mathcal{E}})\mathsf{E}r(t + \tau_0), t \in [0, T_R]$. In practice, we consistently estimate $\mathsf{E}r(t)$ by averaging successive segments of $r(t)$ of duration MT_s to form

$$\bar{r}(t) = \frac{1}{N} \sum_{q=0}^{N-1} r(t + qMT_s), \qquad t \in [0, MT_s]. \quad (7)$$

Using $\bar{r}(t)$ in place of $\mathsf{E}r(t)$, we can readily obtain estimates of the timing τ_0 and the SAT waveform $p_R(t)$ as follows (see also [7]).

Theorem 1: Under C0)–C4), the timing offset τ_0 and the SAT $p_R(t)$ can be consistently estimated in the presence of AGN, ISI, and MUI, using

$$\hat{\tau}_0 = \arg \max_{\tau\in[0,MT_s)} \int_0^{T_R} \bar{r}^2((t + \tau)_{\mathrm{mod}MT_s}) dt$$

$$\hat{p}_R(t) = \frac{1}{\sqrt{\mathcal{E}}} \bar{r}(t + \hat{\tau}_0), \qquad t \in [0, T_R] \quad (8)$$

where the $(\mathrm{mod}MT_s)$ operation is used because $\bar{r}(t)$ in (7) is estimated over a period of size MT_s whereas the integration in

(8) needs its periodic extension. Under C3-B1), the SAT estimate in (8) must be normalized by θ.

As detailed in [7], $\bar{r}(t)$ can be computed either digitally or in analog form, and the maximization in (8) has to be performed over a finite grid of equispaced candidate offsets. Any desirable resolution can be achieved but the density of the grid is typically constrained in practice by the affordable complexity.

The unified approach offered by Theorem 1 for training-based or blind synchronization and SAT recovery is surprisingly simple if one takes into account its attractive features which are not matched by any existing alternative: Universal applicability to NB, WB, or UWB regimes, in the presence of AGN, ISI, and MUI. Only readily available upper bounds on channel parameters are required, for low-complexity estimation based on sample averaging and energy detection. Neither transmit–receive filters nor channels or spreading codes need to be known, so long as they remain invariant while averaging is performed in (7). Furthermore, it is worth mentioning that the approach works even when phase errors are present at the transmitter, pulse distortions in the propagation channel, and unmodeled dynamics at reception (all these can be lumped into $p_R(t)$ which is allowed to be unknown).

The pros and cons of training-based versus blind alternatives are well known and the choice between the two depends on the application. As we alluded to at the beginning of this section, training acquires timing faster and more reliably but with the blind pattern one does not interrupt transmission and does not sacrifice rate. What is common to the training and blind patterns in C3-T1) and C3-B1) is that they both have the master-node increase power (i.e., "raise its voice") periodically to accomplish synchronization. Fortunately, this increase is small since it is effected in a few symbols and only during the synchronization phase which is short relative to the data transmission phase.

C. SAT-Based Demodulation

Having $\hat{\tau}_0$ and $\hat{p}_R(t)$ available, slave nodes can demodulate using the output of an SAT-based correlator which captures full multipath energy and yields the detection statistic

$$d[k] = \int_0^{T_R} \hat{p}_R(t) r(t + kT_s + \hat{\tau}_0) dt. \qquad (9)$$

Relying on $d[k]$, linear equalization or Viterbi's algorithm can be adopted for demodulation depending on the tradeoff between BER requirements and affordable implementation complexity. To further reduce complexity, one can absorb the ISI and MUI plus AWGN terms at the SAT correlator output into a single colored noise term and proceed with a low-complexity (albeit suboptimal) slicer. In code division multiple access (CDMA) and UWB single or multiuser access with binary symbol transmissions this amounts to demodulating symbols with the sign detector

$$\hat{s}[k] = \text{sign}[d[k]]. \qquad (10)$$

For a single piconet, error performance of the timing estimator in (8) with the blind sync pattern and the SAT-based demodulator in (9) and (10) has been evaluated thoroughly in
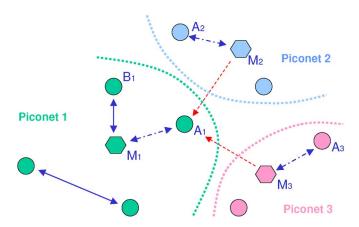

Fig. 3.　WPAN comprising multiple piconets.

[7] and [8], where timing acquisition has been also generalized to nonlinear pulse-position modulations and decision-directed tracking. Whether implemented digitally or as an analog filter, the SAT-based demodulator bypasses the need to perform costly channel estimation. As such, it outperforms the popular RAKE at lower complexity, since even with a reduced number of fingers, the RAKE requires estimation of the channel taps and delays.

Having only a single (namely the master) node broadcasting, either one of the *nonzero* mean patterns [C3-T1) or C3-B1)] enables simultaneous communication with *zero*-mean symbols among already synchronized nodes. This renders our approach robust to MUI both in fixed (e.g., cellular) architectures as well as in *ad hoc* networks with cluster-heads or gateways acting as synchronizers. In cellular CDMA systems for example, the base station can synchronize a user regardless of the MUI present—a challenging problem welcoming such a low-complexity training or blind solution. Likewise, our synchronization and low-complexity demodulation algorithms are welcome in *ad hoc* access systems and WSNs in particular, where resources and cost are at a premium. Our approach in this section requires only a single node transmitting the sync pattern at a time. If two or more sync patterns are "in the air," which is possible when multiple piconets operate simultaneously, each sync pattern can still be extracted by separating piconets in the frequency-domain. But since this requires extra coordination and bandwidth, we are motivated to look for better alternatives in the ensuing section.

III. SYNCHRONIZATION WITHIN MULTIPLE PICONETS

Simultaneous broadcasting of multiple nonzero-mean sync patterns violates C4) and requires redesigning the sync protocol as well as the operating conditions of Section II. Indeed, sync patterns asynchronously broadcasted by multiple master nodes collide and cause what we henceforth term sync-pattern interference (SPI) to receiving slave nodes; see, e.g., Fig. 3 showing three such piconets. For this reason, beyond AGN, ISI, and zero-mean MUI, a desirable protocol should be also resilient to nonzero-mean SPI. To appreciate the difficulty in ensuring SPI resilience through, e.g., piconet-specific spreading sequences, it suffices to recall that despreading requires synchronization; and since the asynchronism among master nodes is allowed to

be arbitrary, designing spreading codes which are (even approximately) orthogonal to all possible shifts is clearly impractical because the required bandwidth is prohibitively large.

Instead of (de)spreading, our idea in this section is to design training patterns with *variable periods* specific to each piconet-u and corresponding receivers with averaging operations specific to each piconet-u to suppress SPI and enable multipiconet synchronization and SAT recovery. To this end, let $\mathcal{N}_p$ denote the number of piconets interfering the reception of a slave node under consideration. Supposing that all piconets $u \in [1, \mathcal{N}_p]$ adopt the same symbol period T_s, we can express the receive waveform as

$$r_u(t) = \sum_{v=1}^{\mathcal{N}_p} r_{uv}(t) + \rho_u(t) + \eta_u(t)$$

$$r_{uv}(t) := \sqrt{\mathcal{E}_v} \sum_n s_v[n] p_{R,uv}(t - nT_s - \tau_{0,uv}) \quad (11)$$

where $r_{uv}(t)$ is the waveform received at any slave node of piconet-u as a result of the sync pattern transmitted by the master node of piconet-v; $\rho_u(t)$ denotes the MUI present at any node of piconet-u which originates from slave nodes of the same or other piconets; and $\eta_u(t)$ is the AGN at the slave node of piconet-u under consideration.[1] Further, $s_v[n]$ stands for the symbol stream transmitted from the master node of piconet-v; $p_{R,uv}(t) := p_{T,v}(t) \star h_{uv}(t + \tau_{0,uv}) \star \tilde{p}_u(t)$ denotes the corresponding waveform from piconet-v received at any node of piconet-u, where $p_{T,v}(t)$ is the symbol waveform transmitted by the master of piconet-v, and $h_{uv}(t)$ models the channel from the master node of piconet-v to this receiving node of piconet-u with time delay $\tau_{0,uv}$. We suppose that C0) and C2) of Section II still hold with proper modifications in notation, but we replace C1) by the following.

C1u) With an upper bound on the delay spread of all channels involved known (and thus with the nonzero support $T_{R,uv}$ of $p_{R,uv}(t)$ also known $\forall u, v \in [1, \mathcal{N}_p]$), we select the integer $M := \max_{u,v} \{ \lceil T_{R,uv}/T_s \rceil \} + 1$.

As in Section II, C1u) will allow us to cope with ISI. To mitigate SPI, we will need to modify also our sync patterns, starting with the training-based ones, as follows.

C3-Tu) The master node of the piconet-u will transmit $s_u[n] = \sum_k f_u[k]\delta[n - kM]$, where $f_1[k] = 1 \forall k$ [i.e., piconet-1 will simply use C3-T1) as before]; but for $u > 1$, the sequence $f_u[k]$ will be chosen periodic with period $Q_u \in \mathbb{N}$ satisfying three conditions. 1) Period Q_u is even $\forall u \in [2, \mathcal{N}_p]$. 2) If $Q_v > Q_u$, then Q_v/Q_u is even $\forall u, v \in [2, \mathcal{N}_p]$. 3) Sequence $f_u[k]$ is binary valued with $f_u[k] = 1$ for $k \in [0, (Q_u/2) - 1]$, and $f_u[k] = -1$ for $k \in [Q_u/2, Q_u - 1]$.

Also, we can modify C4) as follows.

C4u) Only the master node per piconet can transmit the nonzero mean (NZM) sync pattern. As a result, $\rho_u(t)$ and $\eta_u(t)$ in (11) are zero mean, i.e., $\mathsf{E}[\rho_u(t)] = \mathsf{E}[\eta_u(t)] = 0, \forall u \in [1, \mathcal{N}_p]$.

[1]As a mnemonic, symbols with a single-piconet subscript pertain to transmit or receive quantities of the indicated piconet, while for symbols with two subscripts, the first subscript signifies the receiving piconet and the second one denotes the piconet of the transmitting node.

Clearly, the constant sequence $f_1[k] = 1$ of piconet-1 can also be viewed as periodic with period $Q_1 = 1$. Furthermore, we will see that selecting $f_u[k]$ periodic with even period $Q_u, \forall u \in [1, \mathcal{N}_p]$, will allow us through proper averaging operations over periods of size $Q_u M T_s$ to eliminate SPI at receiving slave nodes. This will be also facilitated by condition 3) which dictates an equal number of $+1$s and -1s (hence, zero mean) per period, and also by condition 2) which basically asserts that the period of any piconet's sync pattern should either be an even multiple of another piconet's smaller period, or it should yield another piconet's larger period after being multiplied by an even number. Finally, our motivation behind binary-valued $f_u[k]$ samples is twofold: Constant modulus and simplicity in averaging operations.

As an example of periods satisfying C3-Tu), consider the set

$$Q_u = 2^{u-1} \qquad \forall u \in [1, \mathcal{N}_p]. \quad (12)$$

Notice though that there are more possibilities if one is willing to increase the periods assigned beyond $2^{\mathcal{N}_p - 1}$, e.g., there is no need to consider all the periods in the geometrically increasing set of (12), but select members with periods higher than $2^{\mathcal{N}_p - 1}$.

Conditions 1)-3) under C3-Tu) endow the periodic $f_u[k]$ with three nice properties [P1)–P3)] that will prove handy in suppressing SPI; see the Appendixes A and B for their proofs. The first one will be useful for slave nodes of piconet-1 to suppress SPI from piconets-$u, u > 1$.

P1) If N_1 is a multiple of Q_u and $u > 1$, then for any integer shift m, it holds for the sequences obeying C3-Tu) that $\sum_{q=0}^{N_1 - 1} f_u[q + m] = 0$.

The second property will enable slave nodes of each piconet $u > 1$ to recover the sync pattern of their master node.

P2) For all integers m and q, with $u > 1$, it holds for the sequences obeying C3-Tu) that $f_u[m + qQ_u/2] = (-1)^q f_u[m]$.

The third property will allow slave nodes of a piconet-$u > 1$ to suppress SPI originating from the master node of a piconet-v with larger period training pattern.

P3) For $u, v > 1$, if $Q_v/Q_u = 2Q$ with $Q \in \mathbb{N}$ and $\mathrm{mod}(Q_u, 2) = 0$, then $\forall m \in \mathbb{Z}$, it holds for the sequences obeying C3-Tu) that $\sum_{q=0}^{4Q-1} (-1)^q f_v[m + qQ_u/2] = 0$.

Before proceeding, let us substitute the sync pattern of piconet-v [cf. C3-Tu) with $u = v$] into (11) and use the Kronecker delta definition to obtain

$$r_{uv}(t) = \sqrt{\mathcal{E}_v} \sum_k f_v[k] p_{R,uv}(t - kMT_s - \tau_{0,uv}). \quad (13)$$

Using P1)–P3) and this last expression of $r_{uv}(t)$, we will show next how the C3-Tu) sync patterns with proper operations at receiving slave nodes can suppress SPI.

A. Suppression of SPI

To eliminate SPI in (11), each slave node of say piconet-u should perform an operation enabling recovery of the signal $r_{uu}(t)$ from its own master node and annihilation of the signals $r_{uv}(t)$ from other masters $v \neq u$. We have already seen

in Section II that sample averaging segments of size MT_s as in (7) allows recovery of piconet-1's master-node pattern in the absence of SPI. This will be used also here (after adding subscripts 1 for notational consistency) along with the following receive operations for piconets-u with $u \in [2, \mathcal{N}_p]$.

C3-Ru) Slave nodes of piconet-1 will perform averaging as in (7), i.e.,

$$\bar{r}_1(t) = \frac{1}{N_1} \sum_{q=0}^{N_1-1} r_1(t + qMT_s), \qquad t \in [0, MT_s]. \quad (14)$$

Slave nodes of piconet-u for all $u \in [2, \mathcal{N}_p]$ will perform

$$\bar{r}_u(t) = \frac{1}{N_u} \sum_{q=0}^{N_u-1} (-1)^q r_u \left(t + q \frac{Q_u}{2} MT_s \right) \quad (15)$$

for $t \in [0, Q_u MT_s]$. The number of segments averaged in (14) and (15) are selected to satisfy the following conditions: 1) N_1 must be a multiple of $Q_u \ \forall u > 1$; 2) N_u must be even $\forall u > 1$; and 3) for $Q_v > Q_u$ and $u, v > 1$, N_u must be an even multiple of Q_v/Q_u.

As an example of the number of segments averaged by slave nodes, consider the set

$$N_1 = \mathcal{N}_0 2^{\mathcal{N}_p-1}$$
$$N_u = \mathcal{N}_0 2^{\mathcal{N}_p-u+1} \qquad \forall u \in [2, \mathcal{N}_p] \quad (16)$$

for some $\mathcal{N}_0 \in \mathbb{N}$. We can readily verify that with, e.g., the set of periods in (12), the set in (16) satisfies conditions 1)–3) under C3-Ru). Notice also that although the size of the periods increases with u, the number of segments averaged decreases with u. Hence, the overall time duration it takes to perform the averaging operations in (14) and (15) is the same for all piconets, i.e., $\forall u > 1$, $N_u(Q_u/2)MT_s = \mathcal{N}_0 2^{\mathcal{N}_p-1}MT_s = N_1 MT_s$.

Having specified the training patterns broadcasted by the master node of each piconet in C3-Tu) and the corresponding operations performed by the receiving slave nodes of each piconet in C3-Ru), we are ready to show how their combination enables SPI suppression. Starting with piconet-1, we already know from (5) that $\bar{r}_1(t)$ can recover the pattern of piconet-1, i.e., for $t \in [0, MT_s]$

$$\frac{1}{N_1} \sum_{q=0}^{N_1-1} r_{11}(t + qMT_s) = \sqrt{\mathcal{E}_1} \sum_m p_{R,11}(t - mMT_s - \tau_{0,11}).$$

Proposition 1 shows that $\bar{r}_1(t)$ can also suppress SPI from all other piconets-u with $u \in [2, \mathcal{N}_p]$.

Proposition 1: Under C0), C1u), C2), C3-Tu), and C3-Ru), slave nodes of piconet-1 can annihilate SPI from piconet-u, $\forall u \in [2, \mathcal{N}_p]$, i.e.,

$$\frac{1}{N_1} \sum_{q=0}^{N_1-1} r_{1u}(t + qMT_s) = 0, \quad t \in [0, MT_s] \qquad \forall u \in [2, \mathcal{N}_p].$$

Proof: Using (13) with $u = 1$ and $v = u$, we can write

$$\frac{1}{N_1} \sum_{q=0}^{N_1-1} r_{1u}(t + qMT_s)$$
$$= \frac{\sqrt{\mathcal{E}_u}}{N_1} \sum_{q=0}^{N_1-1} \sum_k f_u[k] p_{R,1u}(t - kMT_s - \tau_{0,1u} + qMT_s)$$
$$= \frac{\sqrt{\mathcal{E}_u}}{N_1} \sum_{q=0}^{N_1-1} \sum_m f_u[m+q] p_{R,1u}(t - mMT_s - \tau_{0,1u})$$
$$= \sqrt{\mathcal{E}_u} \sum_m p_{R,1u}(t - mMT_s - \tau_{0,1u}) \frac{1}{N_1} \sum_{q=0}^{N_1-1} f_u[m+q]$$
$$= 0$$

where for the second equality, we used the change of variables $m := k - q$, and in obtaining the last equality we relied on property P1). [Recall also that P1) requires N_1 to be a multiple of Q_u, thus justifying the need for condition 1) under C3-Ru)]. ∎

Switching roles, we also need to prove that a slave user in piconet-u, $u \neq 1$, can recover the pattern of its own master node while eliminating SPI from the master node of piconet-1.

Proposition 2: Under C0), C1u), C2), C3-Tu), and C3-Ru), slave nodes of piconet-u can annihilate SPI from piconet-1 while being able to recover the training signal from their own master node of piconet-$u \forall u \in [2, \mathcal{N}_p]$, i.e., for $t \in [0, Q_u MT_s]$, we have

$$\bar{r}_{u1}(t) := \frac{1}{N_u} \sum_{q=0}^{N_u-1} (-1)^q r_{u1} \left(t + q \frac{Q_u}{2} MT_s \right)$$
$$= 0$$
$$\bar{r}_{uu}(t) := \frac{1}{N_u} \sum_{q=0}^{N_u-1} (-1)^q r_{uu} \left(t + q \frac{Q_u}{2} MT_s \right)$$
$$= \sqrt{\mathcal{E}_u} \sum_k f_u[k] p_{R,uu}(t - kMT_s - \tau_{0,uu}).$$

Proof: To suppress interference from piconet-1, set $v = 1$ in (8) and (13) to deduce that $r_{u1}(t) = \sqrt{\mathcal{E}_1} \sum_k p_{R,u1}(t - kMT_s - \tau_{0,u1})$. Upon plugging the latter into the averaging operation performed by slave nodes of piconet-u with $u > 1$, we find that for $t \in [0, Q_u MT_s]$

$$\bar{r}_{u1}(t) := \frac{1}{N_u} \sum_{q=0}^{N_u-1} (-1)^q \sqrt{\mathcal{E}_1} \sum_k p_{R,u1}$$
$$\times \left(t - kMT_s + q \frac{Q_u}{2} MT_s - \tau_{0,u1} \right)$$
$$= \left[\sqrt{\mathcal{E}_1} \sum_m p_{R,u1}(t - mMT_s - \tau_{0,u1}) \right]$$
$$\times \left[\frac{1}{N_u} \sum_{q=0}^{N_u-1} (-1)^q \right]$$
$$= 0$$

where the last equality follows because the last term in square brackets is zero for N_u even, thus justifying the need for condition 2) under C3-Ru).

To prove recovery of the training signal from the master node of piconet-u, we use (8) and (13) with $v = u$ and plug the resultant $r_{uu}(t)$ into the averaging operation to obtain

$$
\begin{aligned}
\bar{r}_{uu}(t) :=\; & \frac{\sqrt{\mathcal{E}_u}}{N_u} \sum_{q=0}^{N_u-1} (-1)^q \sum_k f_u[k] p_{R,uu} \\
& \times \left(t - kMT_s + q\frac{Q_u}{2}MT_s - \tau_{0,uu} \right) \\
=\; & \frac{\sqrt{\mathcal{E}_u}}{N_u} \sum_{q=0}^{N_u-1} (-1)^q \sum_m f_u \left[m + q\frac{Q_u}{2} \right] \\
& \times p_{R,uu} \left(t - mMT_s - \tau_{0,uu} \right) \\
=\; & \sqrt{\mathcal{E}_u} \sum_m \left[p_{R,uu} \left(t - mMT_s - \tau_{0,uu} \right) \right. \\
& \left. \times \frac{1}{N_u} \sum_{q=0}^{N_u-1} (-1)^q f_u \left[m + q\frac{Q_u}{2} \right] \right] \\
=\; & \sqrt{\mathcal{E}_u} \sum_m f_u[m] p_{R,uu} \left(t - mMT_s - \tau_{0,uu} \right)
\end{aligned}
$$

for $t \in [0, Q_u MT_s]$, where the last equality follows from property P2). ∎

To this point, we have shown through Propositions 1 and 2 how slave nodes of any piconet can recover the training signal of their own master node. We have also proved that interference to and from piconet-1 can be suppressed under C3-Tu) and C3-Ru). What is left to establish is SPI suppression to and from piconet-u for any $u > 1$. This is accomplished in Proposition 3.

Proposition 3: Under C0), C1u), C2), C3-Tu), and C3-Ru), slave nodes of piconet-u can annihilate SPI from piconet-v and vice versa, i.e., for $v \neq u$ and $\forall u, v \in [2, \mathcal{N}_p]$

$$
\bar{r}_{vu}(t) := \frac{1}{N_v} \sum_{q=0}^{N_v-1} (-1)^q r_{vu} \left(t + q\frac{Q_v}{2}MT_s \right) = 0
$$

$$
\bar{r}_{uv}(t) := \frac{1}{N_u} \sum_{q=0}^{N_u-1} (-1)^q r_{uv} \left(t + q\frac{Q_u}{2}MT_s \right) = 0.
$$

Proof: Recalling condition 3) under C3-Tu) and supposing w.l.o.g. that $Q_v > Q_u$, we can use $Q_v = 2QQ_u$ to rewrite $\bar{r}_{vu}(t)$ as

$$
\begin{aligned}
\bar{r}_{vu}(t) =\; & \frac{1}{N_v} \sum_{q=0}^{N_v-1} (-1)^q r_{vu} \left(t + q\frac{Q_v}{2}MT_s \right) \\
=\; & \frac{1}{N_v} \sum_{q=0}^{N_v-1} (-1)^q r_{vu}(t + qQQ_u MT_s)
\end{aligned}
$$

which after invoking (13), with the roles of u and v interchanged, yields

$$
\begin{aligned}
\bar{r}_{vu}(t) =\; & \frac{1}{N_v} \sum_{q=0}^{N_v-1} (-1)^q \sqrt{\mathcal{E}_u} \sum_k [f_u[k] \\
& \times p_{R,vu}(t + qQQ_u MT_s - kMT_s - \tau_{0,vu})] \\
=\; & \frac{1}{N_v} \sum_{q=0}^{N_v-1} (-1)^q \sqrt{\mathcal{E}_u} \sum_m [f_u[m + qQQ_u] \\
& \times p_{R,vu}(t - mMT_s - \tau_{0,vu})] \\
=\; & \sqrt{\mathcal{E}_u} \sum_m \left[p_{R,vu}(t - mMT_s - \tau_{0,vu}) \right. \\
& \left. \times \frac{1}{N_v} \sum_{q=0}^{N_v-1} (-1)^q f_u[m + qQQ_u] \right] \\
=\; & \sqrt{\mathcal{E}_u} \sum_m f_u[m] p_{R,vu}(t - mMT_s - \tau_{0,vu}) \\
& \times \left[\frac{1}{N_v} \sum_{q=0}^{N_v-1} (-1)^q \right] = 0
\end{aligned}
$$

where the last equality follows since N_v is even as per condition 2) under C3-Ru). This shows that piconet-v can cancel SPI from piconet-u.

To establish the converse, we plug (13) into the averaging operation to arrive at

$$
\bar{r}_{uv}(t) = \frac{1}{N_u} \sum_{q=0}^{N_u-1} \left[(-1)^q \sqrt{\mathcal{E}_v} \right. \\
\left. \times \sum_k f_v[k] p_{R,uv} \left(t - kMT_s - \tau_{0,uv} + q\frac{Q_u}{2}MT_s \right) \right]
$$

which upon changing variable to $m := k - qQ_u/2$, yields

$$
\begin{aligned}
\bar{r}_{uv}(t) =\; & \frac{1}{N_u} \sum_{q=0}^{N_u-1} \left[(-1)^q \sqrt{\mathcal{E}_v} \right. \\
& \left. \times \sum_m f_v \left[m + q\frac{Q_u}{2} \right] p_{R,uv} (t - mMT_s - \tau_{0,uv}) \right] \\
=\; & \sqrt{\mathcal{E}_v} \sum_m \left[p_{R,uv} (t - mMT_s - \tau_{0,uv}) \right. \\
& \left. \times \frac{1}{N_u} \sum_{q=0}^{N_u-1} (-1)^q f_v \left[m + q\frac{Q_u}{2} \right] \right].
\end{aligned}
$$

Recall now that $f_v[k]$ is periodic with period $Q_v = 2QQ_u$, and use condition 3) under C3-Ru) to write $N_u = 2\mathcal{J}(Q_v/Q_u) = \mathcal{J}4Q$ for some $\mathcal{J} \in \mathbb{N}$. Using this into the last sum of the previous equation, we deduce from property P3) that

$$
\begin{aligned}
\frac{1}{\mathcal{J}4Q} \sum_{q=0}^{\mathcal{J}4Q-1} (-1)^q f_v \left[m + q\frac{Q_u}{2} \right] \\
= \frac{1}{4Q} \sum_{q=0}^{4Q-1} (-1)^q f_v \left[m + q\frac{Q_u}{2} \right] = 0 \qquad \forall m
\end{aligned}
$$

which completes the proof of the proposition. ∎

B. Timing and SAT Recovery

In Section III-A, we saw that with properly designed training patterns as in C3-Tu) and with operations at receiving nodes adhering to C3-Ru), it is possible to extract the master node's signal in the piconet of interest from the SPI originating from other piconets. In this section, we will use this extracted signal waveform to acquire timing and recover the SAT of interest in the multipiconet setup under consideration.

Since SPI has been suppressed, we can argue as in Theorem 1 to recognize that AGN and MUI are also eliminated asymptotically by the averaging operations C3-Ru) [cf. C4u)]. [Recall that removal of ISI is already guaranteed thanks to C1u).] Specifically, as the averaging size N_1 grows large, $\bar{r}_1(t)$ in (14) converges to $\bar{r}_{11}(t)$ [cf. (11)], which according to Proposition 1 is SPI-free, i.e., $\bar{r}_{11}(t) = \sqrt{\mathcal{E}_1} \sum_m p_{R,11}(t - mMT_s - \tau_{0,11})$. Likewise, as $N_u \to \infty$ we have for any piconet-u that [cf. (11) and Propositions 2 and 3], as $t \in [0, Q_u MT_s]$

$$\bar{r}_u(t) \to \bar{r}_{uu}(t) = \sqrt{\mathcal{E}_u} \sum_k f_u[k] p_{R,uu}(t - kMT_s - \tau_{0,uu}). \tag{17}$$

Based on (17) and mimicking the steps from [7] we used for Theorem 1, we can readily prove the following.

Theorem 2: Under C0), C1u), C2), C3-Tu), C3-Ru), and C4u), the timing offset $\tau_{0,uu}$ and the SAT $p_{R,uu}(t)$ of each piconet $u \in [1, \mathcal{N}_p]$ can be consistently estimated in the presence of AGN, ISI, MUI, and SPI using

$$\hat{\tau}_{0,uu} = \arg \max_{\tau \in [0, MT_s)} \int_0^{T_{R,uu}} \bar{r}_u^2(t + \tau) dt \tag{18}$$

$$\hat{p}_{R,uu}(t) = \frac{1}{\sqrt{\mathcal{E}_u}} \bar{r}_u(t + \hat{\tau}_{0,uu}), \qquad t \in [0, T_{R,uu}]. \tag{19}$$

Because over the interval $[0, Q_u MT_s]$, the waveform $\bar{r}_u(t)$ in (17) actually contains $Q_u/2$ independent shifted replicas of $p_{R,uu}(t)$, it is possible to improve the accuracy of the recovered SAT using instead of (19) the weighted average estimator: For $t \in [0, T_{R,uu}]$

$$\hat{p}_{R,uu}^{(w)}(t) = \frac{1}{\sqrt{\mathcal{E}_u} Q_u/2} \sum_{q=0}^{(Q_u/2)-1} w_k \bar{r}_u(t + \hat{\tau}_{0,uu} + qMT_s) \tag{20}$$

where the weights $w_k := \text{sign}[\int_0^{T_{R,uu}} \hat{p}_{R,uu}(t) \bar{r}_u(t + \hat{\tau}_{0,uu} + kMT_s) dt]$ account for possible sign differences among different SAT replicas and $\hat{p}_{R,uu}(t)$ is the SAT estimate from (19).

As in Section II-C, having $\hat{\tau}_{0,uu}$ and $\hat{p}_{R,uu}(t)$ available, slave nodes in piconet-u can demodulate information symbols using the detection statistic [cf. (9)]

$$d_u[k] = \int_0^{T_{R,uu}} \hat{p}_{R,uu}(t) r_u(t + kT_s + \hat{\tau}_{0,uu}) dt \tag{21}$$

which for binary symbols allows for simple demodulation using the sign detector

$$\hat{s}_u[k] = \text{sign}[d_u[k]]. \tag{22}$$

Since $f_u[k]$ can take either $+1$ or -1 values, when $\tau_{0,uu}$ is outside the interval $[0, MT_s)$, although the estimator in (18) produces a consistent timing estimate, the recovered SAT in (19) or (20) entails a possible sign ambiguity. For example, when $\tau_{0,uu} = (Q_u/2)MT_s + \epsilon$ with $\epsilon \in [0, T_s)$, we will have $\bar{r}_{uu}(t) = \sqrt{\mathcal{E}_u} \sum_k f_u[k - Q_u/2] p_{R,uu}(t - kMT_s - \epsilon)$, which will yield the correct timing offset as $\epsilon = \arg \max_{\tau \in [0, MT_s)} \int_0^{T_{R,uu}} \bar{r}_{uu}^2(t + \tau) dt$. But even with the correct timing ϵ, the recovered SAT will be $\hat{p}_{R,uu}(t) = (1/\sqrt{\mathcal{E}_u}) \bar{r}_{uu}(t + \epsilon) = -p_{R,uu}(t), t \in [0, T_{R,uu}]$, which has its sign reversed relative to the true SAT. For this possible sign ambiguity in the estimated SAT of piconet-$u(u > 1)$, the detected symbols $\{\hat{s}_u[k]\}$ may have a systematic sign error. This ambiguity can certainly be handled using differential PSK modulation ([13, Ch. 5]). Alternatively, we can extend the transmit pattern in order to cope with this sign ambiguity. One simple approach is to append K "+1" symbols $\{s_u[k]\}_{k=0}^{K-1}$ after the training pattern. With the available SAT estimate $\hat{p}_{R,uu}(t)$, we can then use the sign detector in (22) to find $\{\hat{s}_u[k]\}_{k=0}^{K-1}$, and subsequently remove the sign ambiguity by forming the SAT estimate (suppose K is odd)

$$\check{p}_{R,uu}(t) = \hat{p}_{R,uu}(t) \cdot \text{sign}\left[\sum_{k=0}^{K-1} \hat{s}_u[k]\right], \qquad t \in [0, T_{R,uu}]. \tag{23}$$

In the sequel, we will ignore possible sign ambiguities since, if present, they can be resolved using (23).

C. Blind Synchronization

Using the analogy between a deterministic periodic sequence and the periodic mean of a cyclostationary received waveform, Theorem 1 unifies training-based and blind sync patterns for the single-piconet scenario. Using the same analogy, it is evident that our results in Sections III-A and III-B, which relied on the training-based patterns for multipiconet synchronization and SAT recovery, have their counterparts based on blind sync patterns. For blind operation, however, C3-Tu) must be replaced by the following.

C3-Bu) The master node of the piconet indexed by u will transmit

$$\mathsf{E}[s_u[n]] = \theta \sum_k f_u[k] \delta[n - kM] \tag{24}$$

where piconet-1 will use C3-B1) corresponding to $f_1[k] = 1 \; \forall k$, and the deterministic periodic sequence $f_u[k](u > 1)$ as well as its period Q_u must obey conditions 1)–3) identical to those in C3-Tu).

If master nodes broadcast with the sync patterns C3-Bu), then Propositions 1–3 remain valid for N_u sufficiently large and SPI can be suppressed. Formally stated, the law of large numbers implies that for any $u \in [1, \mathcal{N}_p]$, when $t \in [0, Q_u MT_s]$

$$\lim_{N_u \to \infty} \bar{r}_u(t) = \theta \sqrt{\mathcal{E}_u} \sum_k f_u[k] p_{R,uu}(t - kMT_s - \tau_{0,uu}). \tag{25}$$

However, the latter implies that the timing and SAT estimators of Theorem 2 as well as the weighted and sign-compensated

SAT estimators of (20) and (23) can remain operational also in a blind mode. This is quite remarkable because AGN, ISI, MUI, and SPI can be handled without interrupting the broadcast and without bandwidth loss. As our simulations will confirm, at the expense of requiring larger sample sizes for longer averaging, blind estimators can approach the performance of their training-based counterparts.

We will close this section with two remarks.

Remark 1: In this section, we dealt with multiple piconets each with a single master-node broadcasting the sync pattern. However, our results carry over to the uplink operation of a cellular, e.g., CDMA system where multiple (say $\mathcal{N}_u$) *ad hoc* users want to synchronize with a single access point. Viewing these users as the master nodes herein and equipping them with either the C3-Tu) or the C3-Bu) patterns, solves the long-standing problem of synchronizing multiple *arbitrarily* asynchronous users in the presence of ISI and MUI. Notice that because the number of users $\mathcal{N}_u$ seeking synchronization concurrently is typically small (as many as the number of neighboring masters in the multipiconet setup), using $\mathcal{N}_p = \mathcal{N}_u$ in (12) requires periods of reasonable size.

Remark 2: Averaging continuous-time analog waveforms avoids the possibly high sampling rates involved in the UWB regime, but implementing analog delays required to shift successive $r_u(t)$ segments by MT_s multiples [see (14) and (15)] can be challenging. Nonetheless, chips implementing analog delays from 20 to 1000 ns are available [15] but they are costly and have low accuracy and tolerances. On the other hand, when sampling at 1–2 GHz can be afforded, it is possible to store and process $\bar{r}_u(t)$ digitally, which also facilitates the maximization required to find $\hat{\tau}_{0,uu}$ in (18). In Section IV, we elaborate further on this digital approach.

IV. DIGITAL IMPLEMENTATION

Although all previous derivations were carried out in continuous time, all estimators we developed can also be implemented digitally. Indeed, upon sampling $r_u(t)$ in (11) every T_0 seconds, we obtain

$$
\begin{aligned}
r_u[k] &= \sum_{v=1}^{\mathcal{N}_p} \sqrt{\mathcal{E}_v} \sum_n s_v[n] p_{R,uv}(kT_0 - nK_sT_0 - \Delta_{0,uv}T_0) \\
&\quad + \rho_u(kT_0) + \eta_u(kT_0) \\
&= \sum_{v=1}^{\mathcal{N}_p} \sqrt{\mathcal{E}_v} \sum_n s_v[n] p_{R,uv}[k - nK_s - \Delta_{0,uv}] \\
&\quad + \rho_u[k] + \eta_u[k]
\end{aligned}
\tag{26}
$$

where for notational simplicity we have assumed that $T_s = K_sT_0$ with $K_s \in \mathbb{N}$, and $\tau_{0,uv} = \Delta_{0,uv}T_0$ with $\Delta_{0,uu} \in \mathbb{N}$. Over the time interval $[qMT_s, (q+1)MT_s]$, we can collect the samples of $r_u(t)$ in a vector $\mathbf{r}_u(q) := [r_u[qMK_s], r_u[qMK_s+1], \ldots, r_u[(q+1)MK_s - 1]]^T$. Based on $\mathbf{r}_u(q)$, the receiver of any slave node in piconet-1 will form the average

$$
\bar{\mathbf{r}}_1 = \frac{1}{N_1} \sum_{q=0}^{N_1-1} \mathbf{r}_1(q).
\tag{27}
$$

Likewise, the receiver of any slave node in piconet-u, $u \in [2, \mathcal{N}_p]$, will form

$$
\bar{\mathbf{r}}_u = \frac{1}{N_u} \sum_{q=0}^{N_u-1} (-1)^q \left[\mathbf{r}_u^T\left(q\frac{Q_u}{2}\right), \mathbf{r}_u^T\left(q\frac{Q_u}{2}+1\right), \ldots, \right.
$$
$$
\left. \times \mathbf{r}_u^T\left(q\frac{Q_u}{2} + Q_u - 1\right) \right]^T.
\tag{28}
$$

We can then select Q_u as, e.g., in (12) and N_u as, e.g., in (16) in order to suppress SPI and recover the signal from the piconet of interest using either C3-Bu) or C3-Tu) patterns as established by Propositions 1–3. Then, we can estimate the digital timing $\Delta_{0,uu} \in [0, MK_s - 1]$ using

$$
\hat{\Delta}_{0,uu} = \arg\max_{\Delta \in [0,MK_s-1]} \|\bar{\mathbf{r}}_u(\Delta : \Delta + K_{R,uu})_{\mathrm{mod}Q_uMK_s}\|^2
\tag{29}
$$

where $T_{R,uu} = K_{R,uu}T_0$ and we have used Matlab's notation $\mathbf{x}(i_1 : i_2)$ to denote the subvector formed by the i_1 through i_2 entries of a vector $\mathbf{x}$. With timing acquired, we can recover $\mathbf{p}_{R,uu} := [p_{R,uu}[0], \ldots, p_{R,uu}[K_{R,uu}]]^T$, corresponding to the SAT of piconet-u, as

$$
\hat{\mathbf{p}}_{R,uu} = \frac{1}{\sqrt{\mathcal{E}_u}} \bar{\mathbf{r}}_u((\hat{\Delta}_{0,uu} : \hat{\Delta}_{0,uu} + K_{R,uu})_{\mathrm{mod}Q_uMK_s}).
\tag{30}
$$

After timing acquisition and SAT recovery, we can form similar to (21) the decision statistic

$$
\begin{aligned}
d_u[k] = [r_u[\hat{\Delta}_{0,uu} + kK_s], \ldots, \\
r_u[\hat{\Delta}_{0,uu} + kK_s + K_{R,uu}]] \cdot \hat{\mathbf{p}}_{R,uu}
\end{aligned}
$$

based on which we can proceed with a slicer or more elaborate demodulation schemes such as zero-forcing, minimum mean-square error or maximum-likelihood multiuser detectors.

Remark 3: As far as the sampling rate $(1/T_0)$ is concerned, we can either use Nyquist or sub-Nyquist sampling which corresponds to approximating the integral in the detection statistic [cf. (21)] with a large step size T_0 to form $d_u[k]$. Another option is to filter the received waveform before sampling so that Nyquist rate is affordable. For example, we can have a frond-end 500 MHz bandpass filter and sample its output at 1-GHz rate. Certainly, demodulation performance in this case is traded off for relaxed sampling requirements.

Remark 4: Because the channel is changing with time, our averaging time should be limited to a small fraction of the channel coherent time. As discussed in [4], the anticipated speed of moving users in a typical UWB scenario is about $v = 1$ m/s, which implies that the rate of channel variation is upper bounded by 3 ns/s. With maximum carrier frequency $f_c = 6$ GHz, the maximum Doppler spread is: $f_D = v/(c/f_c) = (6 \times 10^9)/(3.0 \times 10^8) = 20$ Hz. The channel coherence time is then about [14, Ch. 4]: $T_{\mathrm{coh}} = 0.423/f_D = 21$ ms. For the UWB system that we will simulate in Section V, the symbol period is $T_s = 330$ ns. We will have about $\lceil T_{\mathrm{coh}}/T_s \rceil = 64\,000$ symbols within one coherence period. As we will see in the ensuing section, only a small fraction of this coherence period suffices for our multipiconet synchronization and demodulation algorithms.
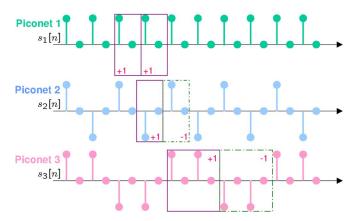
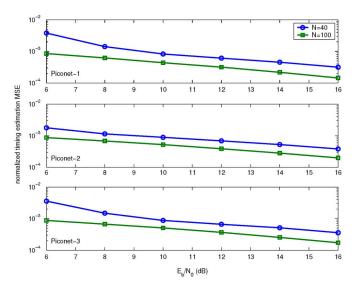Fig. 4.   SPI-resilient training patterns ($M = 2$) as in C3-Tu).

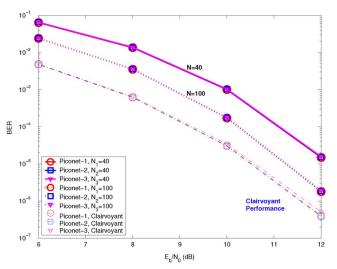Fig. 5.   MSE performance of training-based timing estimation.

Fig. 6.   BER performance with training-based timing and SAT recovery compared against the clairvoyant system where perfect timing and channel knowledge are assumed.
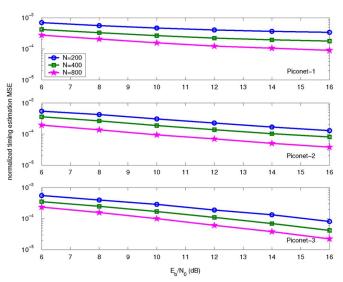

Fig. 7.   MSE performance of blind timing estimation.

V. SIMULATED PERFORMANCE

In this section, we present simulations to evaluate the performance of the novel synchronization protocols and the resultant SAT-based demodulators in a WPAN consisting of $\mathcal{N}_p = 3$ piconets, as shown in Fig. 3. Throughout, we will use BPSK modulation and a pulse shaper (monocycle) equal to the second derivative of the Gaussian bell, i.e., $p(t) = \mathcal{A}[1 - 2t^2/\tau_g^2]e^{-t^2/\tau_g^2}$, where $\mathcal{A}$ is chosen so that $\int_0^{T_p} p^2(t)dt = 1$. By selecting $\tau_g = 0.17$ ns, the nonzero support of $p(t)$ is approximately 1 ns. For each node, the receive filter $\check{p}(t)$ is matched to $p(t)$. The multipath channel model adopted is "CM1" defined by the IEEE 802.15.3 as a working group [5], which has mean excess delay 4.9 ns and root-mean-square (rms) delay spread 5 ns. We have verified experimentally that the delay spread of CM1 is effectively upper bounder by 29 ns. After truncation to 29 ns, the channel is normalized to have unit total power gain. We further select $T_s = 330$ ns, $T_f = 30$ ns, $N_f = 10$, and $T_c = 3$ ns. The TH spreading code $\{c_k\}_{k=1}^9$ for the master node in each piconet is randomly generated taking values in $\{0, 1, \ldots, 9\}$. Clearly, the parameter M can be chosen to be 2 here because we have $T_{R,uv} < T_s, \forall u, v \in \{1, 2, 3\}$. In the following simulations, we choose a sampling period $T_0 = 0.1$ ns to approximate the

performance of the equivalent analog processor. All error-performance curves are averaged over 1000 random channel realizations.

Test 1 (training-based synchronization): For the $\mathcal{N}_p = 3$ piconets, we used the C3-Tu) sequences depicted in Fig. 4 for $M = 2$, and tested the timing estimators in (18) through its digital counterpart in (29). Fig. 5 shows the resultant normalized (with respect to T_s^2) mean-square error (mse) of the timing estimator as a function of the received bit-energy-to-noise ratio for different averaging sizes. The implied BER using the sign detector in (22) is plotted in Fig. 6 for each of the three piconets. In generating these curves, we have simulated the interference power level identical to that of the desired signal.

Test 2 (blind synchronization): Using the same pattern functions $f_u[k]$ implied from Fig. 4 in (24) with $\theta = 1$, we simulated the blind counterpart of the previous test case. Fig. 7 depicts the normalized mse of the blind timing estimate for each of the three piconets, with variable averaging sizes. The resulting detection performance per piconet is plotted in Fig. 8. We have also tested
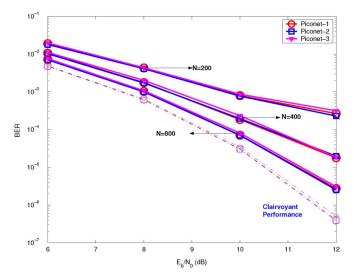
Fig. 8. BER performance with blind timing and SAT recovery compared against the clairvoyant system where perfect timing and channel knowledge are assumed.
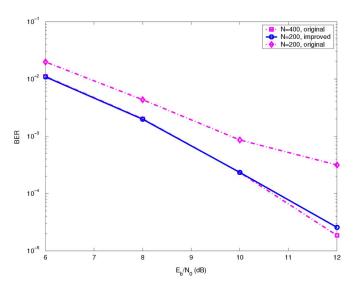

Fig. 9. BER performance with the blind estimate in (20) for the SAT corresponding to piconet-3.

detection performance with the improved SAT estimator in (20). Fig. 9 depicts the resulting BER for piconet-3, where we can clearly see the noise reduction achieved.

VI. CONCLUSION

We introduced low-complexity protocols for timing acquisition and demodulation of asynchronous transmissions in a single or multiple piconets, where nodes are allowed to communicate in the presence of noise, intersymbol, interpiconet, and intrapiconet interference. The novel protocols rely on pattern signals transmitted by the synchronizing node of each piconet and corresponding simple averaging operations performed at receiving nodes to suppress interference and extract the desirable sync pattern. Following a unifying approach, we designed sync patterns for training-based and blind operation. The transmitted signal in the training mode, or its mean in the blind mode, comprise a train of equispaced Kronecker deltas modulated by a binary-valued pattern sequence which

periodically alters the transmit-power with a period unique to each piconet. Receiver processing can be performed either digitally or with analog components.

Exploiting judiciously planned transmit-power variations offers an innovative approach to synchronization. Power increase can be kept to minimal levels by increasing the amount of averaging required at the receiver to estimate the timing offset and the demodulation template. More important, this increase is small since it is present in a few symbols and only during the synchronization phase.

Our focus in this paper has been on UWB piconets of a WPAN or UWB sensor networks, where ISI and MUI effects are severe, timing is of paramount importance, and complexity as well as cost constraints are particularly stringent. For these applications, our training-based algorithms offer speed in acquisition and reliable timing estimates even with short data records, while our blind algorithms provide complementary strengths in bandwidth efficiency, reduced overhead for coordination and uninterrupted operation. Simulations corroborated the potential of both approaches by evaluating their performance in terms of mse of the timing estimates and the resultant BERs in demodulation.

Beyond UWB radios, it is important to stress the universal applicability of our protocols to synchronizing a broad spectrum of NB or WB communication systems and *ad hoc* networks operating in the presence of (possibly heavy) interference. We will highlight the long-standing problem of timing *completely* asynchronous users accessing the base station of a cellular system in severe MUI and/or ISI environments. Our training-based and blind sync patterns are very attractive in this context, since designing spreading sequences which are nearly orthogonal for arbitrary shifts is clearly out of question.

APPENDIX A
PROOF OF PROPERTIES 1 AND 2

The proof of P1) follows directly from condition 3) in C3-Tu) which wants in every period of size Q_u, the sequence $f_u[k]$ to have equal number of -1's and $+1$'s; and since N_1 contains multiple periods, the result is immediate.

To prove P2), recall that condition 1) in C3-Tu) forces Q_u to be even, while 3) implies that $f_u[m] = (-1)f_u[m+1\cdot Q_u/2] = (-1)^2 f_u[m + 2 \cdot Q_u/2] = \cdots = (-1)^q f_u[m + q \cdot Q_u/2]$ for any integer q.

APPENDIX B
PROOF OF PROPERTY 3

Proof: From the division identity, we can write any integer m as $m = lQ_u/2 + \epsilon$ with remainder $\epsilon \in [0, (Q_u/2) - 1]$, and thus

$$\sum_{q=0}^{4Q-1} (-1)^q f_v \left[m + q \frac{Q_u}{2} \right] = \sum_{q=0}^{4Q-1} (-1)^q f_v \left[(q+l)\frac{Q_u}{2} + \epsilon \right].$$

Now note that regardless of the specific value ϵ takes, the summand $f_v[(q+l)(Q_u/2)+\epsilon]$ is invariant with respect to ϵ because over successive intervals of size $Q_u/2$, the periodic sequence $\{f_v[k]\}$ is constant (taking values equal to either $+1$ or -1 over

such intervals) [cf. condition 3) in C3-Tu)]. For this reason, we can set w.l.o.g. $\epsilon = 0$ and seek a proof of

$$\sum_{q=0}^{4Q-1} (-1)^q f_v \left[(q+l) \frac{Q_u}{2} \right] = 0 \qquad \forall l \in \mathbb{Z}. \qquad (31)$$

We will prove (31) by induction on integer l. Since $Q_v = 2QQ_u$, we have for $l = 0$ that $f_v[qQ_u/2] = 1$ when $q \in [0, 2Q-1]$, and $f_v[qQ_u/2] = -1$ when $q \in [2Q, 4Q-1]$. Hence, (31) is satisfied for $l = 0$, since $\sum_{q=0}^{4Q-1} (-1)^q f_v[qQ_u/2] = 0$.

Supposing that (31) holds for some $l \geq 0$, i.e., $\sum_{q=0}^{4Q-1} (-1)^q f_v[(q+l)Q_u/2] = 0$, we want to show that (31) is true for $l+1$, i.e., we wish to show that the sum

$$\sum_{q=0}^{4Q-1} (-1)^q f_v \left[(q+l+1) \frac{Q_u}{2} \right] = \sum_{m=1}^{4Q} (-1)^{m-1} f_v \left[(m+l) \frac{Q_u}{2} \right]$$

is zero (the equality follows after changing variables to $m = q+1$). However, after splitting the last sum, we readily see that

$$\begin{aligned}
&\sum_{m=1}^{4Q} (-1)^{m-1} f_v \left[(m+l) \frac{Q_u}{2} \right] \\
&= (-1) \cdot \sum_{m=0}^{4Q-1} (-1)^m f_v \left[(m+l) \frac{Q_u}{2} \right] \\
&\quad + f_v \left[l \frac{Q_u}{2} \right] - f_v \left[(l+4Q) \frac{Q_u}{2} \right] \\
&= 0
\end{aligned} \qquad (32)$$

where we have used the induction assumption to zero the first term, and the fact that $f_v[k]$ is periodic with period $Q_v = 2QQ_u$, which implies that $f_v[lQ_u/2] = f_v[(lQ_u/2) + Q_v] = f_v[(l+4Q)Q_u/2]$ and nulls the difference between the last two $f_v[\cdot]$ terms. This completes the induction and the proof of P3). ∎

REFERENCES

[1] J. C. Chen, K. Yao, and R. E. Hudson, "Source localization and beamforming," *IEEE Signal Process. Mag.*, vol. 19, no. 2, pp. 30–39, Mar. 2002.

[2] R. Djapic, G. Leus, and A.-J. van der Veen, "Blind synchronization in asynchronous UWB networks based on the transmit-reference scheme," in *Proc. Asilomar Conf. Signals, Syst., Comput.*, Pacific Grove, CA, Nov. 2004, pp. 1506–1510.

[3] E. A. Homier and R. A. Scholtz, "Rapid acquisition of ultra-wideband signals in the dense multi-path channels," in *Proc. Conf. Ultra-Wideband Syst. Technol.*, Baltimore, MD, May 20–23, 2002, pp. 105–110.

[4] IEEE P802.15 Working Group for WPANs, "Time variance for UWB wireless channels" IEEE P802.15-02/461r1-SG3a, Nov. 2002.

[5] IEEE P802.15 Working Group for WPANs, "Channel modeling subcommittee report final" IEEE P802.15-02/368r5-SG3a, Nov. 2002.

[6] V. Lottici, A. D. Andrea, and U. Mengali, "Channel estimation for ultra-wideband communications," *IEEE J. Sel. Areas Commun.*, vol. 20, no. 9, pp. 1638–1645, Dec. 2002.

[7] X. Luo and G. B. Giannakis, "Low-complexity blind synchronization and demodulation for (ultra-) wideband multi-user ad hoc access," *IEEE Trans. Wireless Commun.*, vol. 5, no. 7, pp. 1930–1941, Jul. 2006.

[8] X. Luo and G. B. Giannakis, "Cyclic-mean based synchronization and efficient demodulation for UWB ad hoc access: Generalizations and comparisons," *EURASIP J. Signal Process.*, vol. 89, pp. 2139–2152, Sep. 2006.

[9] I. Maravic, J. Kusuma, and M. Vetterli, "Low-sampling UWB channel characterization and synchronization," *J. Commun. Netw.*, vol. 5, no. 4, pp. 319–327, Dec. 2003.

[10] U. Mengali and A. D. Andrea, *Synchronization Techniques for Digital Receivers*.   New York: Plenum, 1997.

[11] I. Oppermann, L. Stoica, A. Rabbachin, Z. Shelby, and J. Haapola, "UWB wireless sensor networks: UWEN—A practical example," *IEEE Commun. Mag.*, vol. 42, no. 12, pp. S27–S32, Dec. 2004.

[12] D. Porrat and D. Tse, "Bandwidth scaling in ultra wideband communication," presented at the 41st Allerton Conf., Monticello, IL, Oct. 1–3, 2003.

[13] J. G. Proakis, *Digital Communications*, 4th ed.   New York: McGraw-Hill, 2000.

[14] T. S. Rappaport, *Wireless Communications—Principles and Practice*, 2nd ed.   Englewood Cliffs, NJ: Prentice-Hall, 2001.

[15] RCD Components Inc. [Online]. Available: http://216.153.156.169:8080/rcd/rcdpdf/P1410-P2420.pdf

[16] Z. Tian and G. B. Giannakis, "BER sensitivity to mistiming in ultra-wideband communications," *IEEE Trans. Signal Process.*, vol. 53, no. 4, pp. 1550–1560, Apr. 2005.

[17] Z. Wang and X. Yang, "Blind channel estimation for ultra wide-band communications employing pulse position modulation," *IEEE Signal Process. Lett.*, vol. 12, no. 7, pp. 520–523, Jul. 2005.

[18] L. Yang and G. B. Giannakis, "Ultra-wideband communications: An idea whose time has come," *IEEE Signal Process. Mag.*, vol. 21, no. 6, pp. 26–54, Nov. 2004.

[19] L. Yang and G. B. Giannakis, "Timing UWB signals using dirty templates," *IEEE Trans. Commun.*, vol. 53, no. 11, pp. 1952–1963, Nov. 2005.

[20] G. T. Zhou, M. Viberg, and T. McKelvey, "A first-order statistical method for channel estimation," *IEEE Signal Process. Lett.*, vol. 10, no. 2, pp. 57–60, Mar. 2003.

Xiliang Luo (S'03–M'06) received the B.S. degree in physics from Peking University, Beijing, China, in 2001 and the M.S. and Ph.D. degrees in electrical engineering from the University of Minnesota, Minneapolis, in 2003 and 2006, respectively.

In 2006, he joined Qualcomm Inc., San Diego, CA, where he is currently working on the long-term evolution of 3G. His general research interests lie in signal processing, communication, and information theory.

Georgios B. Giannakis (S'84–M'86–SM'91–F'97) received the Diploma in electrical engineering from the National Technical University of Athens, Athens, Greece, in 1981 and the M.Sc. degree in electrical engineering, M.Sc. degree in mathematics, and Ph.D. degree in electrical engineering from the University of Southern California (USC), Los Angeles, in 1983, 1986, and 1986, respectively.

After lecturing for one year at USC, he joined the University of Virginia in 1987, where he became a Professor of Electrical Engineering in 1997. Since 1999, he has been a Professor with the Department of Electrical and Computer Engineering, University of Minnesota, Minneapolis, where he now holds an ADC Chair in Wireless Telecommunications. His general interests are in the areas of communications and signal processing, estimation and detection theory, time-series analysis, and system identification—subjects on which he has authored or coauthored more than 200 journal papers, 350 conference papers, and two edited books. His current research focuses on transmitter and receiver diversity techniques for single and multiuser fading communication channels, complex-field and space–time coding, multicarrier, ultrawideband wireless communication systems, cross-layer designs, and sensor networks.

Dr. Giannakis is the corecipient of six paper awards from the IEEE Signal Processing (SP) and Communications Societies (1992, 1998, 2000, 2001, 2003, 2004). He also received the IEEE SP Society's Technical Achievement Award in 2000. He served as an Editor-in-Chief for the IEEE SIGNAL PROCESSING LETTERS, Associate Editor for the IEEE TRANSACTIONS ON SIGNAL PROCESSING and the IEEE SIGNAL PROCESSING LETTERS, Secretary of the SP Conference Board, member of the SP Publications Board, member and Vice-Chair of the Statistical Signal and Array Processing Technical Committee, Chair of the SP for Communications Technical Committee, and member of the IEEE Fellows Election Committee. He has also served as a member of the IEEE-SP Society's Board of Governors, the Editorial Board for the PROCEEDINGS OF THE IEEE, and the Steering Committee of the IEEE TRANSACTIONS ON WIRELESS COMMUNICATIONS.